

Phase diagram of the one-dimensional extended attractive Hubbard model for large nearest-neighbor repulsion

A. A. Aligia

*Comisión Nacional de Energía Atómica,
Centro Atómico Bariloche and Instituto Balseiro, 8400 S.C. de Bariloche,
Argentina.*

(Received October 5, 2018)

We consider the extended Hubbard model with attractive on-site interaction U and nearest-neighbor repulsions V . We construct an effective Hamiltonian H_{eff} for hopping $t \ll V$ and arbitrary $U < 0$. Retaining the most important terms, H_{eff} can be mapped onto two XXZ models, solved by the Bethe ansatz. The quantum phase diagram shows two Luttinger liquid phases and a region of phase separation between them. For density $n < 0.422$ and $U < -4$, singlet superconducting correlations dominate at large distances. For some parameters, the results are in qualitative agreement with experiments in $\text{Ba}_{1-x}\text{K}_x\text{BiO}_3$.

I. INTRODUCTION

$\text{BaPb}_{1-x}\text{Bi}_x\text{O}_3$ and $\text{Ba}_{1-x}\text{K}_x\text{BiO}_3$ are superconductors with transition temperatures T_c near 13K^1 and 30K^2 respectively. In spite of the fact that these systems do not contain Cu and are non-magnetic³, they have important similarities with the cuprate superconductors, like the perovskite structure, relatively high T_c and low density of states at the Fermi level³. While the electron-phonon interaction is very important in these materials, as shown by inelastic neutron measurements⁴, and the existence of displacements of O atoms and lattice distortions⁵⁻⁷, several other experiments suggest that the pairing mechanism is, at least in part, of electronic nature³. Excitons combined with O displacements^{8,9}, and on-site attractive interaction U based on non-linear screening^{10,11}, have been proposed as the origin of superconductivity in doped BaBiO_3 . In these approaches, repulsive interactions at finite distances play an important role, what is consistent with poor screening of Coulomb interactions by the low density of carriers.

As first shown by Rice and Sneddon¹², treating the displacements d of O ions in the direction of their nearest-neighbor Bi ions in the antiadiabatic approximation, leads to a decrease in U by zg^2/K , and an increase of the repulsion V between nearest Bi atoms by g^2/K , where z is the coordination number, g the electron-phonon interaction, and K the second derivative of the elastic energy with respect to d . This leads naturally to the extended Hubbard model for the description of doped BaBiO_3 , and to superconductivity carried by bipolarons (a pair of carriers at Bi sites accompanied by O displacements)^{12,13}. While the excitonic mechanism involves partial occupation of O states by holes⁸, in agreement with optical experiments¹⁴⁻¹⁶, it is still possible that this one-band model describes the low-energy physics (as in the cuprates¹⁷). This is certainly the case in the purely elec-

tronic model proposed by Varma, in which non-linear screening not only reduces the bare atomic $U \sim 11\text{ eV}$, but renders it negative¹⁰.

In recent years, the phase diagram of the extended Hubbard model in one dimension has been studied by numerical techniques, with particular emphasis in the quarter filled case (number of particles per site $n = 1/2$)¹⁸⁻²⁴. For $n = 1/2$ or $n = 2/3$, $V > 5$ and small negative U , calculations of the correlation exponent K_ρ in systems of up to $L = 16$ sites, predict a Luttinger liquid phase with dominant superconducting correlations at large distances^{19,20}. However, from an analysis based on the infinite V limit and the extrapolation of the spin gap, Penc and Mila suggested that the results of K_ρ were affected by finite-size effects, and the system would not be a Luttinger liquid in that region¹⁹. For $n = 1/2$, perturbative arguments around the infinite V limit (developed in more detail here) suggested that this region corresponds to phase separation²². Monte Carlo studies in systems with $L \sim 64$ lattice sites²³ have shown that the region of phase separation in the model extends to much lower values of V than those obtained for $L \leq 16$, leaving practically no place for a Luttinger liquid phase with dominant superconducting correlations for large V . The extent of this phase remains unclear. Furthermore, due to the above mentioned finite-size effects, and technical problems with different Monte Carlo methods²³, the region of small $|U|$ and $V > 8t$, where t is the hopping, is practically inaccessible to the present available numerical methods. This region is also out of the range of applicability of the continuum-limit field theory (also called g -ology), which has been applied to the extended Hubbard and related models²⁵⁻²⁸.

In this work, we study the one-dimensional attractive Hubbard model in the limit $V \gg t$. Extending previous work¹⁹, we derive an effective low-energy Hamiltonian including terms up to second order in t . Under certain approximations, which are not essential for sufficiently

large V , the effective Hamiltonian is mapped into two XXZ models, representing the movements of particles in singly and doubly occupied sites respectively. From the Bethe ansatz solution of these models, the phase diagram in the thermodynamic limit $L \rightarrow \infty$ as a function of n , $U/t < 0$ and large V/t is obtained. In the next Section, we explain the model and the mapping procedures. The results are shown in Section III. Section IV contains the conclusions and a discussion of the possible relation between our results and the phase diagram measured in $\text{Ba}_{1-x}\text{K}_x\text{BiO}_3$ ⁷.

II. MODEL AND EFFECTIVE HAMILTONIAN

The one-dimensional extended Hubbard Hamiltonian in standard notation is:

$$H = -t \sum_{i\sigma} (c_{i+1\sigma}^\dagger c_{i\sigma} + \text{H.c.}) + U \sum_i n_{i\uparrow} n_{i\downarrow} + V \sum_i n_{i+1} n_i, \quad (1)$$

and we consider the case $U < 0$, $V \gg t$. In this limit, there are no nearest-neighbor occupied sites in the low-energy subspace. The terms in Eq. (1) which mix states of this subspace with states with non-zero occupancy at nearest-neighbor sites, can be eliminated through a standard canonical transformation, as described in Ref.¹⁹. This procedure originates terms of order t^2/V or smaller in the low-energy subspace. The resulting effective Hamiltonian within this subspace (a projector $P = \prod_{i\sigma\sigma'} (1 - n_{i\sigma} n_{i+1\sigma'})$ is implicit) can be written in the form:

$$H_{eff} = H_s + H_d + H_{sd}, \quad (2)$$

where H_s involves only singly occupied sites:

$$\begin{aligned} H_s = & -t \sum_{i\sigma} (c_{i+1\sigma}^\dagger c_{i\sigma} + \text{H.c.}) (1 - n_{i\bar{\sigma}}) (1 - n_{i+1\bar{\sigma}}) \\ & + V_s \sum_{i\sigma\sigma'} n_{i\sigma} n_{i+2\sigma'} (1 - n_{i\bar{\sigma}}) (1 - n_{i+2\bar{\sigma}}) \\ & + V_s \sum_{i\sigma\sigma'} (c_{i+3\sigma}^\dagger c_{i+2\sigma} c_{i+1\sigma'}^\dagger c_{i\sigma'} + \text{H.c.}), \end{aligned} \quad (3)$$

with $V_s = -t^2/V$. The second term is an interaction between second nearest neighbors, and the third term displaces two next-nearest-neighbor particles one lattice parameter.

The second term in Eq. (2) can be described entirely in terms of the operators $d_i^\dagger = c_{i\uparrow}^\dagger c_{i\downarrow}^\dagger$, which create ‘‘doublons’’ at each site:

$$\begin{aligned} H_d = & \Delta_d \sum_i d_i^\dagger d_i - t_d \sum_{i\sigma} (d_{i+1}^\dagger d_i + \text{H.c.}) \\ & + V_d \sum_i d_{i+2}^\dagger d_{i+2} d_i^\dagger d_i, \end{aligned} \quad (4)$$

where $\Delta_d = U - 4t^2/(V - U)$, $t_d = 2t^2/(V - U)$, and $V_d = 4t^2[1/(V - U) - 1/(3V - U)]$ are the effective on-site energy, nearest-neighbor hopping, and next-nearest-neighbor repulsion respectively, for doublons.

The last term in Eq. (2) describes interactions between singly and doubly occupied sites:

$$\begin{aligned} H_{sd} = & M_1 \sum_i [(c_{i+1\uparrow}^\dagger c_{i-1\downarrow}^\dagger + c_{i-1\uparrow}^\dagger c_{i+1\downarrow}^\dagger) \\ & \times (1 - n_{i-1})(1 - n_{i+1})(d_{i-1} + 2d_i + d_{i+1}) + \text{H.c.}] \\ & + M_2 \sum_{i\sigma} (c_{i\sigma}^\dagger d_{i+2}^\dagger d_i c_{i+2\sigma} + \text{H.c.}) \\ & + V_{sd} \sum_{i\sigma\delta=\pm 2} n_{i\sigma} (1 - n_{i\bar{\sigma}}) d_{i+\delta}^\dagger d_{i+\delta}. \end{aligned} \quad (5)$$

Here $M_1 = -t^2[1/V + 1/(V - U)]/2$ describes annihilation of a doublon with creation of two particles at empty sites, and the Hermitian conjugate process, while $M_2 = t^2/(2V - U)$ ($V_{sd} = t^2[2/(V - U) - 2/(2V - U) - 1/(2V)]$) corresponds to interchange (interaction) of a doublon and a particle at a singly occupied next-nearest-neighbor site.

For $V = +\infty$, all terms of H_{eff} vanish except the first term of Eq. (3) and the first term of Eq. (4), and H_{eff} can be solved exactly¹⁹. In this limit, for $U > -4t$ and sufficiently small density n , the system has no doubly occupied sites and is described by H_s . Instead, for $U < -4t$, $n \leq 1$, the ground state of H_{eff} is the same as that of H_d and has no singly occupied sites. For other values of U and $n \leq 1$, the system phase separates into the phases just described, and the limits of the region of phase separation (PS) can be obtained using the Maxwell construction (finding the common tangent to the curves $E_s(n)$ and $E_d(n)$, where $E_\alpha(n)$ is the ground state of H_α at density n).

For the sake of clarity we call ‘‘metallic’’ (M) the phase without double occupancy (ground state of H_s), and ‘‘bipolaronic’’ (BP), the phase described by the ground state of H_d , although the negative U is not necessarily related with atomic displacements in a real system. For finite but large V , the energy cost for constructing a uniform phase with both, singly and doubly occupied sites is high in comparison with M_1 , M_2 and V_{sd} . Thus, in the ground state, H_{sd} can only act in the PS region, at the boundary between M and BP phases, and is irrelevant in the thermodynamic limit. Our main approximation is the neglect of H_{sd} . This should be correct as long as the energy gain of H_s in the PS region ($\sim t$) is larger than the terms of H_{sd} ($\sim t^2/V$). We also neglect the last term of Eq. (3). This term vanishes at the extreme densities of the M phase ($n = 0$ and $n = 1/2$). The ratio of its expectation value with respect to the expectation value of the first term of Eq. (3) can be estimated by perturbation theory:

$$r = \frac{t}{V} [n_s \cos(\pi n_s) - \frac{1}{\pi} \sin(\pi n_s)], \quad (6)$$

where $n_s = n/(1 - n)$. The remaining terms of H_s ,

and the whole of H_d can both be mapped into a spinless fermion model H_α^{sf} ($\alpha = s$ or d):

$$H_\alpha^{sf} = \Delta_\alpha \sum_i f_i^\dagger f_i - t_\alpha \sum_{i\sigma} (f_{i+1}^\dagger f_i + \text{H.c.}) + V_\alpha f_i^\dagger f_i f_{i+1}^\dagger f_{i+1}, \quad (7)$$

with $\Delta_s = 0$. When $\alpha = s$, a site occupied by a fermion f_i^\dagger corresponds to a single occupied site *and* an empty site at the right of it, as explained in detail by Penc and Mila¹⁹ (a similar mapping was also used in a model for oxygen ordering in $\text{YBa}_2\text{Cu}_3\text{O}_{6+x}$ ²⁹). Then, for L sites and N particles in H_s , the corresponding number of sites and particles in H_s^{sf} are $L_s = L - N$, $N_s = N$. Then, the energy per site $e_s(n)$ of H_s for density n is related to the corresponding quantity $e_s^{sf}(n_s)$ of H_s^{sf} by:

$$e_s(n) = \frac{E_s}{L} = \frac{L_s}{L} \frac{E_s^{sf}}{L_s} = (1 - n) e_s^{sf}(n_s). \quad (8)$$

Similarly, H_d can be cast into the form of Eq. (7), mapping a doubly occupied site and an empty site at the right of it into a single site occupied by a fermion. The mapping of the different physical quantities is the same as that used before to find the correlation exponent K_ρ in a generalized $t - J$ model with very large three-site term^{30,31}. The number of sites and fermions in H_d^{sf} are $L_d = L - N/2$, $N_d = N/2$. The energy per site of H_d is given in terms of that of H_d^{sf} by:

$$e_d(n) = (1 - \frac{n}{2}) e_d^{sf}(n_d); \quad n_d = \frac{n}{2 - n}. \quad (9)$$

To calculate K_ρ , we also need the mapping of the velocity³⁰:

$$v_d = \frac{L}{L_d} v_d^{sf} = \frac{2}{2 - n} v_d^{sf}, \quad (10)$$

and/or the Drude weight:

$$D_d = \frac{L}{2} \frac{\partial^2 E_d(\Phi)}{\partial \Phi^2} = 4 \frac{L_d}{L} \frac{\partial^2 E_d^{sf}(\Phi_{sf})}{\partial \Phi_{sf}^2} = 2(2 - n) D_d^{sf}. \quad (11)$$

Here $E_d(\Phi)$ ($E_d^{sf}(\Phi_{sf})$) is the energy of a ring described by H_d (H_d^{sf}) threaded by a flux Φ (Φ_{sf}). The correlation exponent can be calculated as³¹:

$$K_\rho = \frac{\pi v_d}{2\partial^2 e_d / \partial n^2} = \frac{\pi D_d}{v_d} = \pi \left(\frac{D_d}{2\partial^2 e_d / \partial n^2} \right)^{1/2}. \quad (12)$$

Similar expressions give K_ρ for H_s , but we do not give them, since in the M phase always $K_\rho < 1$, and we are interested in the region $K_\rho > 1$, for which superconducting correlations dominate at large distances.

Using a Jordan-Wigner transformation, H_α^{sf} is transformed into an equivalent XXZ model with L_α sites and M_α spins down:

$$H_\alpha^{sf} \equiv H_\alpha^{XXZ} = 2t_\alpha \sum_i (S_i^x S_{i+1}^x + S_i^y S_{i+1}^y) + V_\alpha \sum_i S_i^z S_{i+1}^z + \Delta_\alpha N_\alpha + V_\alpha (N_\alpha - L_\alpha/4). \quad (13)$$

We have calculated the energy $e_\alpha^{sf}(n_\alpha)$ solving numerically the integral equations of the exact Bethe ansatz solution of Eq. (13) in the thermodynamic limit³². To obtain K_ρ , we have calculated the excitation energies for two small momenta, solving numerically the corresponding Bethe ansatz equations³³. This allowed us to extract $v_d^{sf}(n_d)$. From it, the numerical second derivative of $e_d(n)$, Eqs. (9), (10) and the first Eq. (12), K_ρ was calculated for $n_d \neq 1/2$. For $n_d = 1/2$, we had technical problems in the calculation of $v_d^{sf}(n_d)$, but fortunately, analytical expressions are known^{34,35}:

$$v_d^{sf} = \frac{\pi t \sin \mu}{\mu}; \quad D_d^{sf} = \frac{v_d^{sf}}{4(\pi - \mu)}; \quad \mu = \arccos(V/2t). \quad (14)$$

Using Eqs. (10), (11), (12) and (14), one has for $n = 2/3$ ($n_d = 1/2$):

$$K_\rho(2/3) = \frac{4}{9(1 - \mu/\pi)}. \quad (15)$$

For $V_\alpha = 0$, H_α^{sf} can be solved trivially³⁰ and Eqs.(9), (10), (11), (12) lead to another analytical result for $V_d = 0$:

$$K_\rho(2/3) = \frac{(2 - n)^2}{2}. \quad (16)$$

Since always $V_d/t_d > 0$, and K_ρ decreases with increasing V_d , Eq. (16) implies that for large V , no phase with dominant superconducting correlations exists for $n \geq 2 - \sqrt{2} \simeq 0.59$.

III. BETHE ANSATZ RESULTS

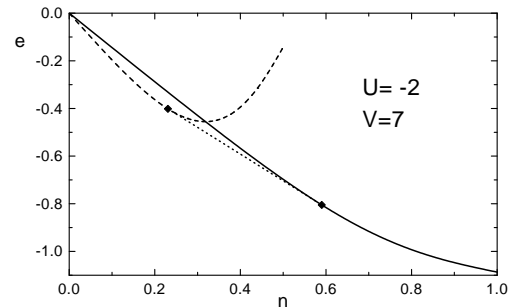


FIG. 1. Ground state energy of the phase with singly occupied sites (dashed line) and doubly occupied sites (full line) as a function of density. The dotted line is the Maxwell construction (see text).

In Fig. 1 we show the energy per site of H_s ($e_s(n)$) with the last term neglected, and that of H_d ($e_d(n)$), as a function of density n for $U = -2$ and $V = 7$. We take $t = 1$ as the unit of energy. The dotted line represents the energy for average composition n , of an inhomogeneous (phase separated) mixture of the “metallic” (M) phase described by H_s for density $n_1 = 0.2307$ and the “bipolaron” (BP) phase (ground state of H_d) for density $n_2 = 0.5901$. These compositions n_i , represented by diamonds in Fig. 1, are obtained finding the common tangent to both curves $e_s(n)$ and $e_d(n)$ (Maxwell construction). Between them, the energy of the phase separated phase is lower than both $e_s(n)$ and $e_d(n)$. The energy $e_s(n)$ is dominated by the first term of Eq. (3), which already exists for $V = +\infty$. The effect of finite large V is small (except near $n = 1/2$ for which the first term of Eq. (3) vanishes), and does not change n_1 significantly. Instead, the effect of a finite large V on n_2 is dramatic, reducing it from $n_2 = 1$ to $n_2 < 0.6$. This is because for $V = +\infty$, $e_d(n)$ is always a straight line (extending from $e_d(0) = 0$ to $e_d(1) = -1$ if $U = -2$). The second and third term of H_d (Eq.(4)), taken into account exactly, are responsible of the curvature of $e_d(n)$ and the shift of n_2 from 1. This is the main effect of finite large V .

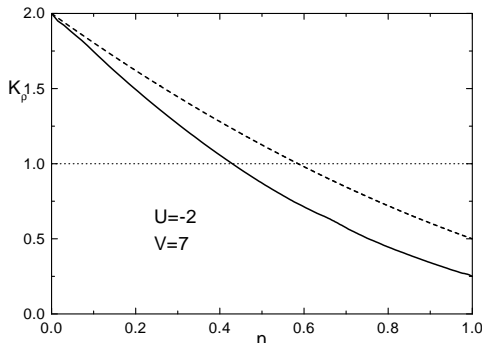


FIG. 2. Correlation exponent K_ρ as a function of density in the “bipolaron” (BP) phase for $U = -2$ and $V = 7$ (full line). The dashed line is the result in absence of the effective nearest-neighbor repulsion between doubly occupied sites ($V_d = 0$).

Another important effect of a finite V is that the pairs acquire mobility and for low densities, superconducting correlations dominate at large distances ($K_\rho > 1$) in the BP phase. In Fig. 2 we represent $K_\rho(n)$ in this phase for the same parameters of Fig. 1. Also shown is the analytical result Eq. (16), which is an upper bound of K_ρ for any values of $U < 0$ and $V \gg t$. For $V \rightarrow +\infty$, we obtain a critical density $n_c = 0.422$ for which $K_\rho(n_c) = 1$. For $n < n_c$ and arbitrary values of $U < 0$ and $V \gg t$, the exponent $K_\rho(n) > 1$. Thus, n_c lies in the interval $(0.422, 2 - \sqrt{2})$. For $-5 \leq U \leq 0$ and $5 \leq V \leq 20$, we find that $n_c < 0.45$. Also, n_c depends very weakly

on U and V within the studied range of parameters, decreasing with increasing repulsions. For $U = -2$, $V = 7$ (as in Figs. 1 and 2), $n_c = 0.429$. These results disagree with those obtained by numerical diagonalization of small systems^{19,20}, which obtained $K_\rho > 1$ for small values of $|U|$, large V and $n = 1/2$, $n = 2/3$, but agree with the statement that the system might not be a Luttinger liquid in that region¹⁹, and with recent Monte Carlo results in larger systems²³. These results and the ones shown below indicate that there is phase separation (PS) in that region. We believe that the reason of the artificially large values of K_ρ in the above mentioned numerical results is that they were calculated using the first Eq. (12) with $\partial^2 e / \partial n^2 = 1/(\kappa n^2)$ determined numerically from the energy for N , $N - 2$ and $N + 2$ particles with $N/L = n$. In phase separated regions (dashed line in Fig. 1), the compressibility κ diverges in the thermodynamic limit, but in small systems, κ can be large and positive due to finite-size effects, leading to very large values of K_ρ , while in fact the system is not a Luttinger liquid. This effect was present in numerical studies of the one-dimensional $t - J$ model with correlated hopping³⁶.

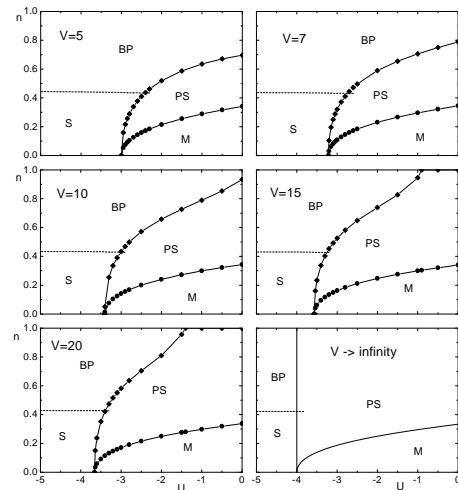


FIG. 3. Phase diagram of the model in the density- U plane, for different values of V . The phase without doubly occupied sites is called “metallic” (M), while the phase with no singly occupied sites is denoted as “bipolaronic” (BP), and if $K_\rho > 1$ we call it “superconducting” (S). The region of phase separation is labeled PS.

In Fig. 3 we show the phase diagram of the model, determined using the Maxwell construction (as in Fig. 1) for different values of U and V (points indicated with solid symbols in Fig. 3), and searching the critical densities n_c for which $K_\rho(n_c) = 1$. The phase diagram for $V \rightarrow +\infty$ was already known, except for the boundary at $n = 0.422$, which separates the BP phase with $K_\rho < 1$ (in which charge correlation functions are the dominant ones at large distances) from the “superconducting” (S) phase with $K_\rho > 1$. The most noticeable effect of a finite V , already present for V as large as $20t$ is the change in the boundary between the BP and PS regions, as a consequence of the above mentioned curvature of $e_d(n)$ for $V < +\infty$. Also, as V decreases, the region S with $K_\rho > 1$ increases, moving to larger values of U and to slightly larger densities. Finally, the PS region is reduced.

The case $V = 5$ is probably beyond the quantitative validity of our large V approximation. Monte Carlo results for $V = 8$ (Fig. 14 of Ref.²³) are in qualitative agreement with our results. Quantitatively, Clay *et al.* obtain that for $U = 0$, phase separation begins at $n_1 \sim 0.5$, while for $V = 7$ we obtain $n_1 = 0.345$. This difference might be due to the effect of terms of order t^m with $m > 2$ or the third term of H_s (Eq. (3)), which we have neglected. Terms of order t^4 reduce t_d and increase n_1 . The limit between S and M phases at low densities is affected neither by H_{sd} (Eq. (5)) nor by the third term of H_s , but might be changed slightly by terms of order t^4 .

IV. SUMMARY AND DISCUSSION

Generalizing a previous approach¹⁹, we have constructed an effective Hamiltonian H_{eff} for the extended Hubbard model when $V \gg t$ and $U \leq 0$. This permits to study the region $V > 8t$, which is outside the region of validity of weak-coupling approaches^{25–28}, while numerical diagonalization of small systems^{19,20,22} display important finite-size effects, as discussed in Section III, and Monte Carlo calculations have some technical problems²³. The effective Hamiltonian can be divided in three parts: H_s , H_d and H_{sd} . The latter is irrelevant for sufficiently large V , and H_s (H_d) acts on a phase in which all particles move in singly (doubly) occupied sites. H_d and the most important terms of H_s were mapped into a Bethe ansatz exactly solvable model, which allows to obtain the energy and correlation exponent K_ρ in the thermodynamic limit. From this information we have constructed the phase diagram. We obtain a region for low and intermediate densities and sufficiently negative U , in which the system behaves as a Luttinger liquid with dominant superconducting correlations at large distances, for any finite $V \gg t$. The existence of this phase and the main changes in the phase diagram with respect to the $V = +\infty$ limit, are due to the dynamics of doubly occupied sites in H_d , controlled by terms of order $t^2/(V - U)$. The most noticeable effect of a finite V for moderate val-

ues of $|U|$ ($U > -4$), is that the upper density of the phase separation (PS) region is reduced from $n = 1$ to much lower values. Instead, the larger density for which superconducting correlations dominate at large distances remains near $n = 0.42$. Thus, the place left by the PS region is mostly occupied by the BP (“bipolaronic” “normal”) phase rather than by the S (“superconducting”) phase. Nevertheless, as V decreases from very large values to $V \sim 7$, the upper value of U for which the S phase exists increases from -4 to ~ -3 .

The extended Hubbard model with attractive U can be justified in different ways, as a model for doped BaBiO₃, as discussed in Section I. In spite of the different dimensionality of the real compound, one can discuss qualitatively the physics expected from the phase diagram (Fig. 3). BaBiO₃ has one electron per site ($n = 1$), and the ground state of the model is a charge density wave, in which nearest-neighbor sites are not equivalent, as experimentally observed^{5–7}. For sufficiently negative U , as n decreases (corresponding to partial replacement of Ba for K) keeping $n_c \sim 0.4 < n < 1$, the ground state of the model is a Luttinger liquid with dominant charge density wave correlations at large distances, with wave vector $2k_F = \pi n$. Experimentally, the ground state of Ba_{1-x}K_xBiO₃ has different charge density wave orderings for $0 \leq x < \sim 0.4$ ($1 \geq n > \sim 0.6$)⁷. As n is further lowered (corresponding to increasing $x = 1 - n$), the model enters a region with dominant superconducting correlations at large distances, which has a corresponding superconducting phase in Ba_{1-x}K_xBiO₃ (for $\sim 0.4 < x < 0.5$)⁷. Above $x = 0.5$ the experimental system cannot be formed, since the solubility limit of K atoms is exceeded. This picture is also consistent with mean-field calculations in the three-dimensional model for different parameters¹⁰.

ACKNOWLEDGMENTS

We are partially supported by CONICET. This work was sponsored by PICT 03-00121-02153 of ANPCyT and PIP 4952/96 of CONICET.

¹ A.W. Sleight, J.L. Gillson, and P.E. Bierstadt, Solid State Commun. **17**, 27 (1975).

² L.F. Mattheiss, E.M. Gyorgy, and D.W. Johnson, Jr., Phys. Rev. B **37**, 3745 (1988); R.J. Cava, B. Battlog, J.J. Krajewski, R. Farrow, L.W. Rupp Jr., A.E. White, K. Short, W.F. Peck, and T. Kometani, Nature (London) **332**, 814 (1988).

³ B. Battlog, R.J. Cava, L.W. Rupp Jr., A.M. Mjusc, J.J. Krajewski, J.P. Remeika, W.F. Peck Jr., A.S. Cooper, and G.P. Espinosa, Phys. Rev. Lett **61**, 1670 (1988).

- ⁴ C.K. Loong, P. Vashishta, R.K. Kalia, M.H. Degani, D.L. Price, J.D. Jorgensen, D.G. Hinks, B. Dabrowski, A.W. Mitchell, D.R. Richards, and Y. Zheng, Phys. Rev. Lett. **62**, 2628 (1989).
- ⁵ D.E. Cox and A.W. Sleight, Acta Crystallogr. B **35**, 1 (1979).
- ⁶ C. Chaillout, A. Santoro, J.P. Remeika, A.S. Cooper, G.P. Espinosa, and M. Marezio, Solid State Commun. **65**, 1363 (1988).
- ⁷ S. Pei, J.D. Jorgensen, B. Dabrowski, D.G. Hinks, D.R. Richards, A.W. Mitchell, J.M. Newsam, S.K. Sinha, D. Vaknin, and A.J. Jacobson, Phys. Rev. B **41**, 4126 (1990).
- ⁸ M.D. Núñez Regueiro and A.A. Aligia, Phys. Rev. Lett. **61**, 1889 (1988); J. Bala and A.M. Oleś, Phys. Rev. B **47**, 515 (1993); A.A. Aligia, M.D. Núñez Regueiro, and E.R. Gagliano, *ibid* **40**, 4405 (1989); A.A. Aligia and M. Balaña, *ibid* **47**, 14380 (1993).
- ⁹ J.O. Sofo, A.A. Aligia, and M.D. Núñez Regueiro, Phys. Rev. B **39**, 9701 (1989); **40**, 6955 (1989).
- ¹⁰ C.M. Varma, Phys. Rev. Lett. **61**, 2713 (1988).
- ¹¹ D. Nguyen Manh, D. Mayou and F. Cyrot-Lackmann, Solid State Commun. **79**, 723 (1991).
- ¹² T.M. Rice and L. Sneddon, Phys. Rev. Lett. **47**, 689 (1981).
- ¹³ R. Micnas, J. Ranninger and S. Robaszkiewicz, Rev. Mod. Phys. **62**, 113 (1990); references therein.
- ¹⁴ S. Salem-Sugui, Jr., E.E. Alp, S.M. Mini, M. Ramanathan, J.C. Campuzano, G. Jennings, M. Faiz, S. Pei, B. Dabrowski, Y. Zheng, D.R. Richards, and D.G. Hinks, Phys. Rev. B **43**, 5511 (1991).
- ¹⁵ S.M. Heald, D. Di Marzio, M. Croft, M.S. Hedge, S. Li, and M. Greenblatt, Phys. Rev. B **40**, 8828 (1989).
- ¹⁶ S. Uchida, S. Tajima, A. Masaki, S. Sugai, K. Kitazawa, and S. Tanaka, J. Phys. Soc. Jpn **54**, 4395 (1985).
- ¹⁷ M.E. Simon, A.A. Aligia, and E. Gagliano, Phys. Rev. B **56**, 5637 (1997); references therein. H. Rosner, H. Eschrig, R. Hayn, S.-L. Drechsler, and J. Málek, *ibid* **56**, 3402 (1997); references therein..
- ¹⁸ F. Mila and X. Zotos, Europhys. Lett. **24**, 133 (1993).
- ¹⁹ K. Penc and F. Mila, Phys. Rev. B **49**, 9670 (1994).
- ²⁰ K. Sano and Y. Ono, J. Phys. Soc. Jpn. **63**, 1250 (1994).
- ²¹ H.Q. Lin, E.R. Gagliano, D.K. Campbell, E.H. Fradkin, and J.E. Gubernatis, in “*The Physics and the Mathematical Physics of the Hubbard Model*”, edited by D. Baeriswyl *et al.* (Plenum, New York, 1995).
- ²² A.A. Aligia, Europhys. Lett. **45**, 411 (1999).
- ²³ R.T. Clay, A.W. Sandvik, and D.K. Campbell, Phys. Rev. B **59**, 4665 (1999).
- ²⁴ M. Nakamura, cond-mat/9909277.
- ²⁵ J. Voit, Phys. Rev. Lett. **64** 323 (1990).
- ²⁶ J.W. Cannon and E. Fradkin, Phys. Rev. B **41**, 9435 (1990).
- ²⁷ J. Voit, Phys. Rev. B **45**, 4027 (1992).
- ²⁸ A.A. Aligia and L. Arrachea, Phys. Rev. B in press (BG7464).
- ²⁹ A.A. Aligia, Phys. Rev. B **47**, 15308 (1993).
- ³⁰ C.D. Batista, F. Lema, and A.A. Aligia, Phys. Rev. B **52**, 6223 (1995).
- ³¹ The correlation exponent K_ρ refers to the original model Eq. (1), and not to the spinless models. In general, the relations defining K_ρ depend on the number of branches around the Fermi level [see for example G. Santoro, N. Manini, A. Parola, and E. Tosatti, Phys. Rev. B **53**, 828 (1996)].
- ³² C.N. Yang and C.P. Yang, Phys. Rev. **150**, 321 (1996); **150**, 327 (1996).
- ³³ M. Fowler and M.W. Puga, Phys. Rev. B **18**, 421 (1978).
- ³⁴ B. Sriram Shastry and B. Sutherland, Phys. Rev. Lett. **65**, 243 (1990).
- ³⁵ T. Giamarchi and A.M. Tsvelik, Phys. Rev. B **59**, 11398 (1999); references therein.
- ³⁶ F. Lema, C.D. Batista, and A.A. Aligia, Physica C **259**, 287 (1996).